Journal of the Korean Crystal Growth and Crystal Technology
Vol. 19, No. 1 (2009) 39-47

Generic studies on thermo-solutal convection of mercurous chloride system of Hg_2Cl_2 and Ne during physical vapor transport

Jeong-Gil Choi, Kyong-Hwan Lee* and Geug-Tae Kim†

Department of Nano-Bio Chemical Engineering, Hannam University, Taejon 305-811, Korea
**Climate Change Technology Research Division, Korea Institute of Energy Research, Taejon 305-343, Korea*

(Received December 9, 2008)
(Accepted January 14, 2009)

Abstract The effects of thermo-solutal convection on mercurous chloride system of Hg_2Cl_2 and Ne during physical vapor transport are numerically investigated for further understanding and insight into essence of transport phenomena. For $10\,K \le \Delta T \le 30\,K$, the growth rate slowly increases and, then is decreased gradually until $\Delta T = 50\,K$. The occurrence of this critical point near at $\Delta T = 30\,K$ is likely to be due to the effects of thermo-physical properties stronger than the temperature gradient corresponding to driving force for thermal convection. For the range of $10\,Torr \le P_B \le 300\,Torr$, the rate is second order-exponentially decayed with partial pressures of component B, P_B. For the range of $5 \le M_B \le 200$, the rate is second order-exponentially decayed with a function of molecular weight of component B, M_B. Like the case of a partial pressure of component B, the effects of a molecular weight are reflected through the binary diffusivity coefficients, which are intimately related with suppressing the convection flow inside the growth enclosure, i.e., transition from convection to diffusion-dominant flow mode as the molecular weight of B increases. The convective mode is near at a ground level, i.e., on earth ($1\ g_0$), and the convection is switched to the diffusion mode for $0.1\ g_0 \le g \le 10^{-2} g_0$, whereas the diffusion region ranges from $10^{-2} g_0$ up to $10^{-5} g_0$.

Key words Mercurous chloride, Thermo-solutal convection, Ne, and physical vapor transport

1. Introduction

Mercurous chloride (Hg_2Cl_2) materials are important for applications in acousto-optic and opto-electronic devices such as Bragg cells, X-ray detectors operating at ambient temperature [1]. The equimolar Hg_2Cl_2 compound decomposes to two liquids at a temperature near 525°C where the vapor pressure is above 20 atm [2, 3]. Because of this decomposition and high vapor pressure, Hg_2Cl_2 cannot be solidified as a single crystal directly from the stoichiometric melt. However, very similar to the mercurous bromide, mercurous chloride exhibits sufficiently high vapor pressure at low temperatures so that these crystals are usually grown by the physical vapor transport (PVT) in closed silica glass ampoules. The PVT processing has many advantages over melt-growth methods since it can be conducted at low temperatures: (1) vapor-solid interfaces possess relatively high interfacial morphological stability against non-uniformities in heat and mass transfer; (2) high purity crystals are achieved; (3) materials decomposed before melting, such as Hg_2Cl_2 can be grown; (4) lower point defect and dislocation densities are achieved [4]. The mechanism of the PVT process is simple: sublimation-condensation in closed silica glass ampoules in temperature gradient imposed between the source material and the growing crystal. In the actual PVT system of Hg_2Cl_2, the molecular species Hg_2Cl_2 sublimes as the vapor phase from the crystalline source material (Hg_2Cl_2), and is subsequently transported and re-incorporated into the single crystalline phase (Hg_2Cl_2) [5]. Recently, PVT has become an important crystal growth process for a variety of acousto-optic materials. However, the industrial applications of the PVT process remain limited. One of important main reasons is that transport phenomena occurring in the vapor are complex and coupled so that it is difficult to design or control the process accurately. Such complexity and coupling are associated with the inevitable occurrence of thermal and/or solutal convection generated by the interaction of gravity with density gradients arising from temperature and/or concentration gradients. In general, convection has been regarded as detrimental and, thus, to be avoided or minimized in PVT growth system. These thermal and/or solutal convection-induced complications result in problems ranging from crystal inhomogeneity to structural imperfection. Therefore, in order to analyze and control the PVT process accurately, and also make significant improvements in the process, it is essen-

†Corresponding author
Tel: +82-42-629-8837
Fax: +82-42-629-8835
E-mail: gtkim@hnu.kr

tial to investigate the roles of convection in the PVT process.

Markham, Greenwell and Rosenberger [6] examined the effects of thermal and thermo-solutal convections during the PVT process inside vertical cylindrical enclosures for a time-independent system, and showed that even in the absence of gravity, convection can be present, causing nonuniform concentration gradients. They emphasized the role of geometry in the analysis of the effects of convection. As such these fundamentally constitute steady state two-dimensional models. The steady state models are limited to low Rayleigh number applications, because the oscillation of the flow field occurs as the Rayleigh number increases. To address the issue of unsteady flows in PVT, Duval [7] performed a numerical study on transient thermal convection in the PVT processing of Hg_2Cl_2 very similar to the mercurous bromide for a vertical rectangular enclosure with insulated temperature boundary conditions for Rayleigh numbers up to 10^6. Nadarajah *et al.* [8] addressed the effects of solutal convection for any significant disparity in the molecular weights of the crystal components and the inert gas. Zhou *et al.* [9] reported that the traditional approach of calculating the mass flux assuming one-dimensional flow for low vapor pressure systems is indeed correct. Rosenberger *et al.* [10] studied three-dimensional numerical modeling of the PVT yielded quantitative agreement with measured transport rates of iodine through octofluorocyclobutane (C_4F_8) as inert background gas in horizontal cylindrical ampoules.

In this theoretical study, a two-dimensional model is used for the analysis of the PVT processes during vapor-growth of mercurous chloride crystals (Hg_2Cl_2) in horizontally oriented, cylindrical, closed ampoules in a two-zone furnace system. Diffusion-limited processes are considered in this paper, although the recent paper of Singh, Mazelsky and Glicksman [11] demonstrated that the interface kinetics plays an important role in the PVT system of Hg_2Cl_2. Thermally buoyancy-driven convection will be considered at this point, primarily for a mixture of Hg_2Cl_2 vapor and impurity of Neon (Ne), although solutally-induced convection is more important than thermal convection in some cases.

It is the purpose of this paper to relate applied thermo-solutal convection process parameters such as such (1) temperature differences between the source and the crystal region, (2) imposed temperature profiles, (3) partial pressures of component B (Ne), (4) molecular weights, (5) gravitational levels and (6) binary diffusivity coefficients to the crystal growth rate and the maximum velocity magnitude to examine the effects of the addition of inert gas (Ne) on thermal and/or solutal buoyancy-driven convection in order to gain insights into the underlying physicochemical processes.

2. Physical and Mathematical Formulations

Consider a rectangular enclosure of height H and transport length L, shown in Fig. 1. The source is maintained at a temperature T_s, while the growing crystal is at a temperature T_c, with $T_s > T_c$. PVT of the transported component A (Hg_2Cl_2) occurs inevitably, due to presence of impurities, with the presence of a component B (Ne). The interfaces are assumed to be flat for simplicity. The finite normal velocities at the interfaces can be expressed by Stefan flow deduced from the one-dimensional diffusion-limited model [12], which would provide the coupling between the fluid dynamics and species calculations. On the other hand, the tangential component of the mass average velocity of the vapor at the interfaces vanishes. Thermodynamic equilibria are assumed at the interfaces so that the mass fractions at the interfaces are kept constant at $\omega_{A,s}$ and $\omega_{A,c}$. On the vertical non-reacting walls appropriate velocity boundary conditions are no-slip, the normal concentration gradients are zero, and wall temperatures are imposed as nonlinear temperature gradients.

Thermo-physical properties of the fluid are assumed to be constant, except for the density. When the Boussinesq approximation is invoked, density is assumed constant except the buoyancy body force term. The density is assumed to be a function of both temperature and concentration. The ideal gas law and Dalton's law of partial pressures are used. Viscous energy dissipation and the Soret-Dufour (thermo-diffusion) effects can be neglected, as their contributions remain relatively insig-

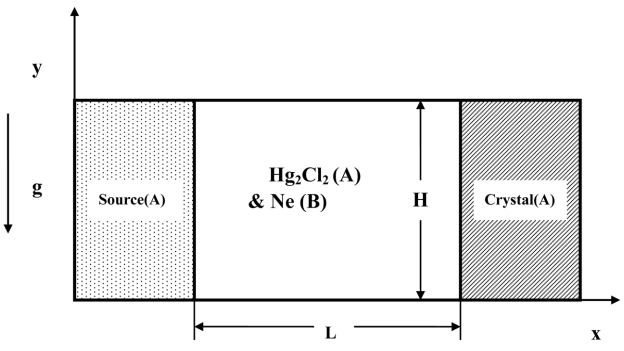

Fig. 1. Schematic of PVT growth reactor in a two-dimensional rectangular system.

nificant for the conditions encountered in our PVT crystal growth processes. Radiative heat transfer can be neglected under our conditions, based on Kassemi and Duval [13].

The transport of fluid within a rectangular PVT crystal growth reactor is governed by a system of elliptic, coupled conservation equations for mass (continuity), momentum, energy and species (diffusion) with their appropriate boundary conditions. Let u_x, u_y denote the velocity components along the x- and y-coordinates in the x, y rectangular coordinate, and let T, ω_A, p denote the temperature, mass fraction of species A (Hg_2Cl_2) and pressure, respectively.

The dimensionless variables are defined as follows:

$$x^* = \frac{x}{H}, \quad y^* = \frac{y}{H}, \tag{1}$$

$$u^* = \frac{u_x}{U_c}, \quad v^* = \frac{u_y}{U_c}, \quad p^* = \frac{p}{\rho_c U_c^2}, \tag{2}$$

$$T^* = \frac{T - T_c}{T_s - T_c}, \quad \omega_A^* = \frac{\omega_A - \omega_{A,c}}{\omega_{A,s} - \omega_{A,c}}. \tag{3}$$

The dimensionless governing equations are given by:

$$\nabla^* \bullet V^* = 0, \tag{4}$$

$$\vec{V}^* \bullet \nabla^* \vec{V}^* = -\nabla^* p^* + Pr\nabla^{*2} V^* - Ra \cdot Pr \cdot T^* \cdot e_g, \tag{5}$$

$$\vec{V}^* \bullet \nabla^* T^* = \nabla^{*2} T^* \tag{6}$$

$$\vec{V}^* \bullet \nabla^* \omega_A^* = \frac{1}{Le} \nabla^{*2} \omega_A^* \tag{7}$$

These nonlinear, coupled sets of equations are numerically integrated with the following boundary conditions:

On the walls ($0 < x^* < L/H$, $y^* = 0$ and 1):

$$u^*(x^*, 0) = u^*(x^*, 1) = v^*(x^*, 0) = v^*(x^*, 1) = 0 \tag{8}$$

$$\frac{\partial \omega_A^*(x^*,0)}{\partial y^*} = \frac{\partial \omega_A^*(x^*,1)}{\partial y^*} = 0,$$

$$T^*(x^*,0) = T^*(x^*,1) = \frac{T - T_c}{T_s - T_c}$$

On the source ($x^* = 0$, $0 < y^* < 1$):

$$u^*(0,y^*) = -\frac{1}{Le(1 - \omega_{A,s})} \frac{\Delta\omega}{\partial x^*} \frac{\partial \omega_A^*(0,y^*)}{\partial x^*}, \tag{9}$$

$$v^*(0, y^*) = 0,$$

$$T^*(0, y^*) = 1,$$

$$\omega_A^*(0, y^*) = 1.$$

On the crystal ($x^* = L/H$, $0 < y^* < 1$):

$$u^*(L/H,y^*) = -\frac{1}{Le(1 - \omega_{A,c})} \frac{\Delta\omega}{\partial x^*} \frac{\partial \omega_A^*(L/H,y^*)}{\partial x^*} \tag{10}$$

$$v^*(L/H, y^*) = 0,$$

$$T^*(L/H, y^*) = 0,$$

$$\omega_A^*(L/H, y^*) = 0.$$

Interfacial velocities (sublimation and condensation velocities) in equations (9) and (10) can also be expressed in terms of a dimensionless Peclet number and a concentration parameter as follows:

$$u(0,y^*) = -\frac{1}{Pe \cdot Ar} \frac{1}{(C_v - 1)} \frac{\partial \omega_A^*(0,y^*)}{\partial x^*} \tag{11}$$

$$u(L/H,y^*) = -\frac{1}{Pe \cdot Ar} \frac{\Delta\omega}{C_v} \frac{\partial \omega_A^*(L/H,y^*)}{\partial x^*} \tag{12}$$

where the Peclet number and concentration parameter C_v are defined as

$$Pe = \frac{u_{adv} L}{D_{AB}}, \quad C_v = \frac{1 - \omega_{A,c}}{\Delta\omega}. \tag{13}$$

The Peclet number can be also estimated by thermodynamic variables:

$$Pe = \ln\left(\frac{p_B(L)}{p_B(0)}\right). \tag{14}$$

U_{adv} is a characteristic velocity which depends on the thermodynamics of physical vapor transport processes, i.e., the vapor pressure of Hg_2Cl_2 as a function of temperature. The mass fraction at the solid-vapor interfaces is fixed at the corresponding temperature. Thus for a given set of conditions, the mass fraction cannot be varied independently. The concentration parameter C_v in equations (11) and (12) represents the ratio of mass fraction. As the Peclet number increases, C_v decreases [18, 19]. The existence of velocities at the interfaces leads to the coupling between the fluid dynamics and species calculations.

In the dimensionless parameters in the governing equations the thermo-physical properties of the gas mixture are estimated from gas kinetic theory using Chapman-Enskog's formulas [16].

The vapor pressure [17] p_A of Hg_2Cl_2 (in the unit of Pascal) can be evaluated from the following formula as a function of temperature: in which a = 29.75, b = 11767.1.

$$p_A = e^{(a - b/T)}, \tag{15}$$

The crystal growth rate V_c is calculated from a mass balance at the crystal vapor interface, assuming fast kinetics, i.e. all the vapor is incorporated into the crys-

tal, which is given by (subscripts c, v refer to crystal and vapor, respectively)

$$\int \rho_v \upsilon_v \cdot ndA = \int \rho_c \upsilon_c \cdot ndA, \tag{16}$$

$$\upsilon_c = \frac{\rho_v \int \upsilon_v \cdot ndA}{\rho_c \int dA}. \tag{17}$$

The detailed numerical schemes in order to solve the discretization equations for the system of nonlinear, coupled governing partial differential equations are found in [18].

3. Results and Discussion

The purposes for this study is to correlate the growth rate and the convective intensity to process parameters such as (1) temperature differences between the source and the crystal region, (2) imposed temperature profiles, (3) partial pressures of component B (Ne), (4) molecular weights, (5) gravitational levels and (6) binary diffusivity coefficients to investigate the effects of inert gas Ne on thermo-solutal convection during physical vapor transport. Thus, it is desirable to express some results in terms of dimensional growth rate, however they are also applicable to parameter ranges over which the process varies in the manner given. The six dimensionless parameters, namely Gr, Ar, Pr, Le, C_v and Pe, are independent and arise naturally from the dimensionless governing equations and boundary conditions. The dimensionless parameters and physical properties for the operating conditions of this study are shown in Table 1.

Table 1
Typical thermo-physical properties used in this study (M_A = 472.086, M_B = 20.183)

Transport length, L	50 cm
Height, H	1 cm
Source temperature, T_s	350°C
Crystal temperature, T_c	300°C
Density, ρ	0.0018 g/cm^3
Dynamic viscosity, μ	0.00032 g/(cm·sec)
Diffusivity, D_{AB}	0.77 cm^2/s
Thermal expansion coefficient, β	0.0016 K^{-1}
Prandtl number, Pr	1.12
Lewis number, Le	0.2
Peclet, Pe	3.45
Concentration number, C_v	1.03
Total system pressure, P_T	443 Torr
Partial pressure of component B, P_B	50 Torr
Thermal Grashof number, Gr	2.24×10^3
Solutal Grashof number, Gr_s	3.77×10^4

Because the molecular weight of a light element (Ne) is not equal to that of the crystal component (Hg_2Cl_2) during the physical vapor transport, both solutal and/or thermal effects should be considered in this study. Also, thermal convection only could be reflected when solutal convection would be assumed to be negligible by setting the molecular weight of component B (Ne) equal to that of the component A, Hg_2Cl_2 at density term in Eq. (5). Both adiabatic and conductive wall boundary conditions are considered. Note it is difficult to obtain the adiabatic wall boundary conditions in practice and most of vapor growth experiments. But, a nonlinear thermal profile ("hump") imposed at the walls is not considered at this point which can be obtained by an often used experimental technique to prevent undesirable nucleations [19, 20]. In general, this temperature hump could eliminate the problem of vapor supersaturation along the transport path and, thus, of parasitic nucleations at the walls. But, these humps may result in sharp temperature gradients near the crystal region, inducing thermal stresses and a decrease in crystal quality.

Fig. 2 shows the growth rates of Hg_2Cl_2 as a function of the temperature difference between the source and the crystal region, ΔT (K), for $10\ K \le \Delta T \le 50\ K$, with insulating boundary walls. For $10\ K \le \Delta T \le 30\ K$, the growth rate slowly increases and, then is decreased gradually until $\Delta T = 50$ K. The occurrence of this critical point near at $\Delta T = 30$ K is likely to be due to the

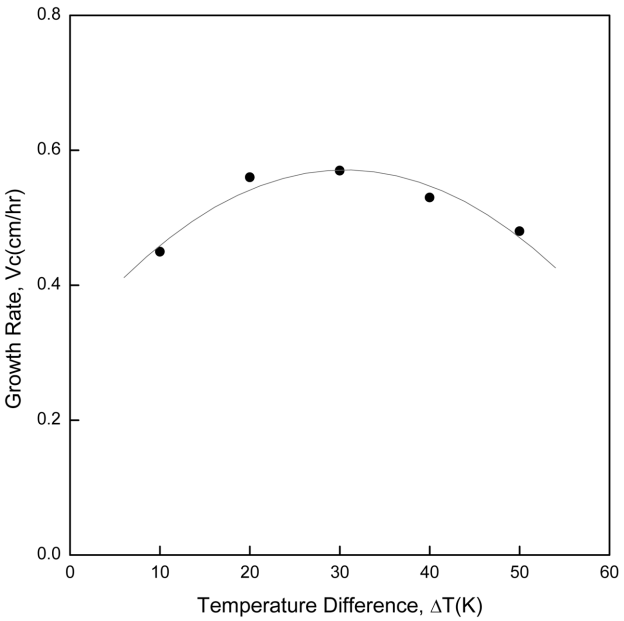

Fig. 2. Growth rates of Hg_2Cl_2 as a function of the temperature difference between the source and the crystal region, ΔT (K), for $10\ K \le \Delta T \le 50\ K$, Ar = 5, P_B = 50 Torr, Ar = 5, L = 5 cm and T_s = 350°C, with the adiabatic walls and thermal convection only.

effects of thermo-physical properties stronger than the temperature gradient corresponding to driving force for thermal convection, as discussed later. Fig. 3 shows the relationship between the Peclet number, Pe and the growth rate, corresponding to Fig. 2. The comparison of Figs. 2 and 3 shows the same pattern and behavior for the growth rate against the temperature difference and the Peclet number. In other words, it means that the temperature is linearly related to the Peclet number whose definition can found in Eqs. (13) and (14). The growth rate exhibits a parabolic behavior against the dimensionless Peclet number, and for $1.2 \le Pe \le 2.5$, the growth rate slowly increases and, then, since at $Pe = 2.6$, is decreased gradually until $Pe = 3.5$. Fig. 4 shows the dimensional maximum velocity magnitude, $|U|_{max}$ is

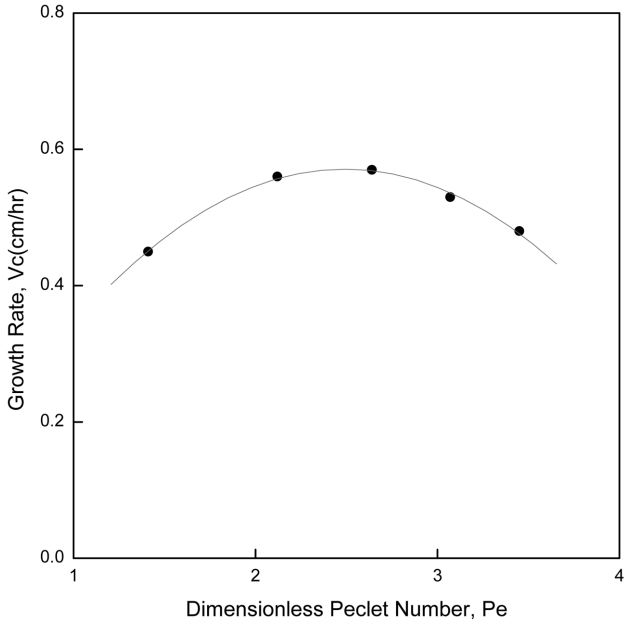

Fig. 3. Relationship between the growth rate and the dimensionless Peclet number, Pe, corresponding to Fig. 2.

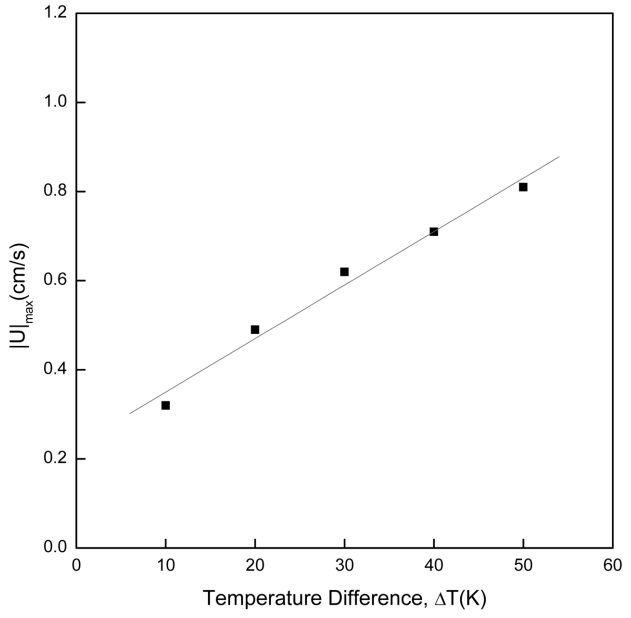

Fig. 4. The $|U|_{max}$ as a function of the temperature difference between the source and the crystal region, $\Delta T(K)$, corresponding to Fig. 2.

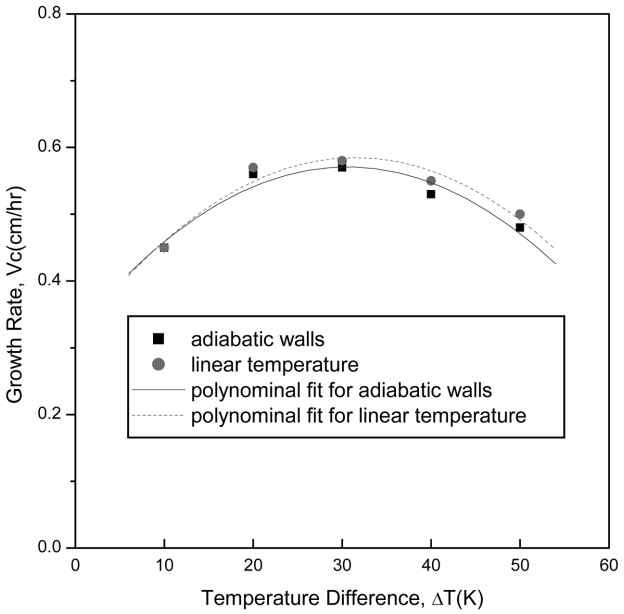

Fig. 5. Effects of wall boundary conditions on the growth rates of Hg_2Cl_2, for $10\,K \le \Delta T \le 50\,K$, $Ar = 5$, $P_B = 50$ Torr, $Ar = 5$, $L = 5$ cm and $T_s = 350^oC$, with thermal convection only, corresponding to Fig. 2.

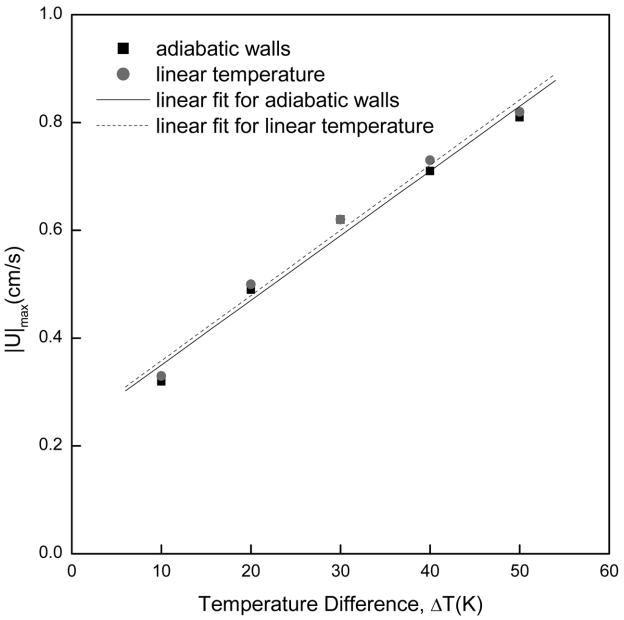

Fig. 6. Effects of wall boundary conditions on the $|U|_{max}$, corresponding to Fig. 5.

proportional to the temperature difference ΔT by a factor of 0.012 cm/s·K, which corresponds to Fig. 2. Note the dimensional maximum velocity magnitude, $|U|_{max}$ implies the importance of intensity of convection during physical vapor transport.

Fig. 5 shows the effects of wall boundary conditions on the growth rates of Hg_2Cl_2 for 10 K ≤ ΔT ≤ 50 K. As shown in Figs. 5 and 6, both the rates and the $|U|_{max}$s for the case of linear temperature profile are slightly greater than for the adiabatic walls for temperature ranges under consideration. For the temperature differences lower than ΔT = 30 K the rates for both cases remain nearly invariant, but with increasing the temperature differences, the rates for the linear walls are more deviated from those for the adiabatic walls. As shown in Fig. 6, with regards to the $|U|_{max}$s, there are no changes between both wall boundary conditions. It would be likely to be due to a diffusion-dominant mode over a convective-dominant mode, as more discussed later. Figs. 2 through 5 are based on Ar = 5, P_B = 50 Torr, 10 K ≤ ΔT ≤ 50 K, P_T = 443 Torr, T_s = 350°C with adiabatic walls and thermal convection in horizontal rectangular enclosures. Note that in general, with a linear temperature profile, the vapor of component A (Hg_2Cl_2) is in a supersaturation throughout the ampoule [21]. As discussed previously, thermal convection only could be considered by setting the molecular weight of component B (Ne) equal to that of the component A, Hg_2Cl_2. It means solutal convection would be assumed to be negligible. For the case of ΔT = 50 K, Ar = 5, P_B = 50 Torr, P_T = 443 Torr, T_s = 350°C with thermal convection only, the corresponding five dimensionless parameters are Pr = 1.12, Le = 0.2, Pe = 3.46, C_v = 1.03, Gr (Grashof number) = 2.42×10^3.

Fig. 7 shows the effects of partial pressures of component B, P_B on the growth rates of Hg_2Cl_2 for 5 Torr ≤ P_B ≤ 300 Torr, for ΔT = 50 K, P_B = 50 Torr, Ar = 5 with adiabatic walls and thermal convection only. The rate is second order-exponentially decayed with partial pressures of component B, P_B for the range of 10 Torr ≤ P_B ≤ 300 Torr. For 10 Torr ≤ P_B ≤ 50 Torr, the rate is decreased significantly by the factor of 0.006, and for 50 Torr ≤ P_B ≤ 300 Torr, reduced by a factor of 0.001. In other words, the decreasing degree is approximately 0.006 for 10 Torr ≤ P_B ≤ 50 Torr, and 0.001 for 50 Torr ≤ P_B ≤ 300 Torr, respectively. The effect of a partial pressure of component B, PB is reflected through the binary diffusivity coefficient, which is intimately related with suppressing the convection flow inside the growth enclosure, i.e., transition from convective mode to diffusion mode as the partial pressures of component B increase. Fig. 8 shows on the uniformities of the growth rates of Hg_2Cl_2 in the interfacial positions, y (cm) as a function of partial pressures of component B, P_B. As the partial pressures of component B increase from P_B = 10 Torr up to 300 Torr, the uniformity of growth rate develops into flatness. Fig. 9 shows the growth rates of Hg_2Cl_2 as a function of molecular weight of component B, M_B with adiabatic walls and thermal convection only. Like the

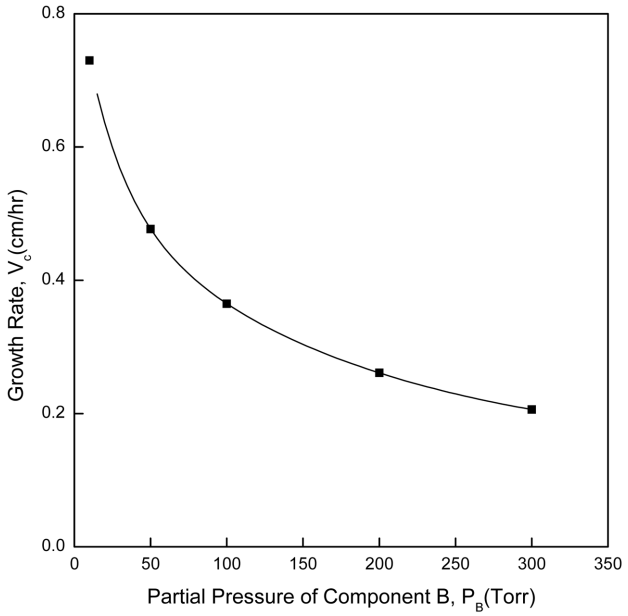

Fig. 7. Effects of partial pressure of component B, P_B (Torr) on the crystal growth rates of Hg_2Cl_2.

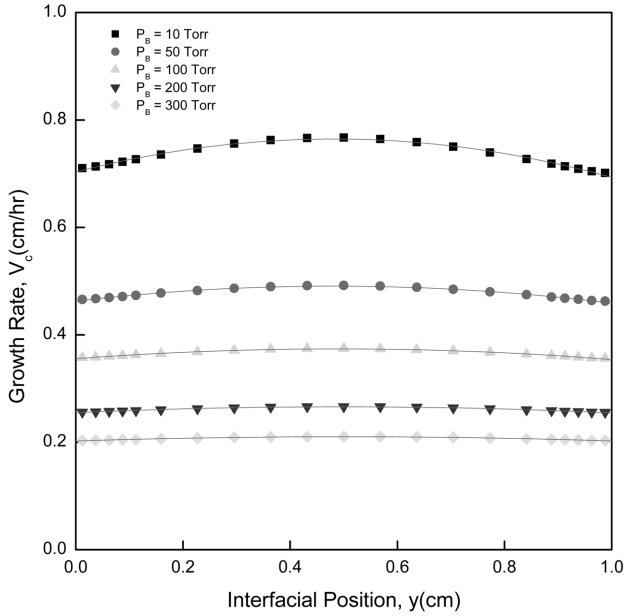

Fig. 8. Interfacial distribution of crystal growth rate of Hg_2Cl_2 for 10 Torr ≤ P_B ≤ 300 Torr, corresponding to Fig. 7.

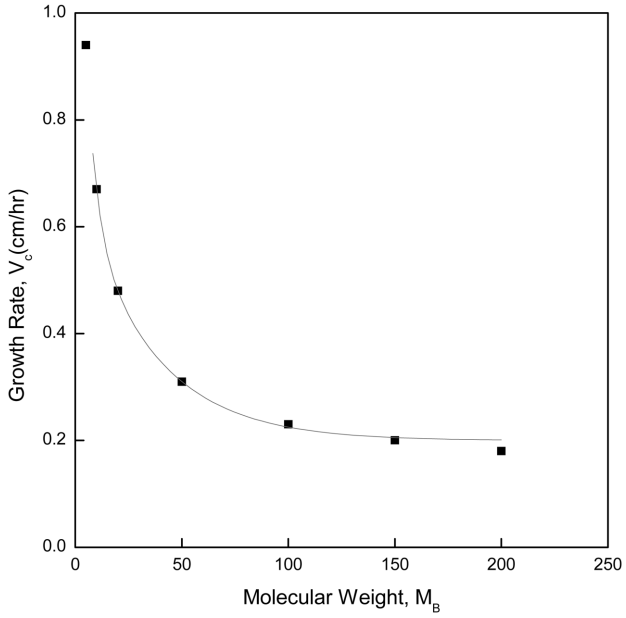

Fig. 9. Effects of molecular weight of component B, M_B on the crystal growth rates of Hg_2Cl_2, for $5 \le M_B \le 200$. Based on $P_B = 50$ Torr, $\Delta T = 50$ K, Ar = 5, L = 5 cm, and $T_s = 350^oC$, with adiabatic walls and thermal convection. Note the density term is dependent on temperature only. Variations of M_B are reflected through the diffusivity coefficient only.

case of Fig. 7, the rate is second order-exponentially decayed with a function of molecular weight of component B, M_B for the range of $5 \le M_B \le 200$. The rate is decreased sharply for the range from $M_B = 5$ to 50 by a factor of 0.014, and then for $50 \le M_B \le 200$, is decreased by a factor of 0.0009. Like the case of a partial pressure of component B, the effects of a molecular weight are reflected through the binary diffusivity coefficients, which are intimately related with suppressing the convection flow inside the growth enclosure, i.e., transition from convection to diffusion-dominant flow mode as the molecular weight of B increases. As shown in Fig. 10, the uniformities of growth rates in the interfacial positions develop into relatively flat shapes from slightly parabolic patterns for the range of $5 \le M_B \le 200$. It implies with increasing the molecular weight of B, the importance of diffusion over convection appears through the binary diffusivities, which could be quantitatively expressed in term of dimensionless Lewis number.

Fig. 11 illustrates the effects of gravitational levels on the transport phenomena within enclosures. For the dimensional maximum velocity magnitude, $|U|_{max}$s, $1g_0 \le g \le 10^{-5}g_0$, the convective mode is near at a ground level, i.e., on earth (1 g_0). The transition mode is switched from the convection to the diffusion mode for $0.1g_0 \le g \le 10^{-2}g_0$, whereas the diffusion region ranges from $10^{-2}g_0$ up to $10^{-5}g_0$. The dimensional maximum velocity magnitude, $|U|_{max}$ drops dramatically from 1.0 cm/s at $1g_0$ down to 0.6 cm/s at $0.1g_0$, which corresponds to nearly 40% off. Fig. 12 shows the uniformities of growth rate in the interfacial positions for both $g = 1g_0$ and $0.1g_0$. For the case of $g = 1g_0$, the shape is not symmetrical at

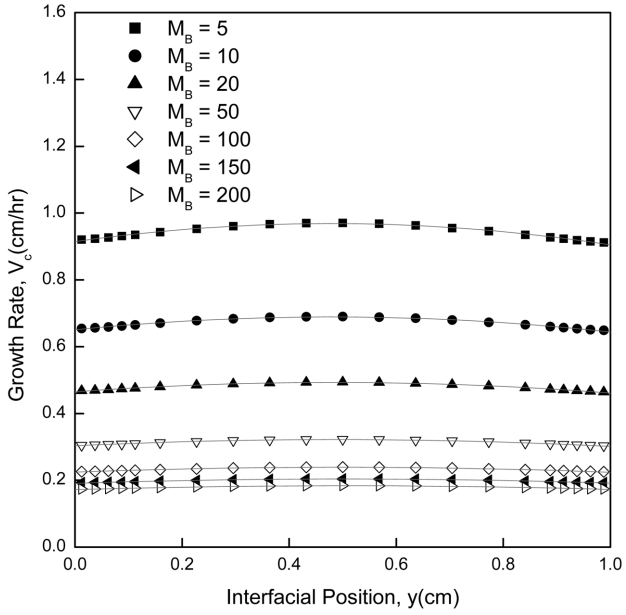

Fig. 10. Interfacial distribution of crystal growth rate of Hg_2Cl_2 for $5 \le M_B \le 200$, corresponding to Fig. 9.

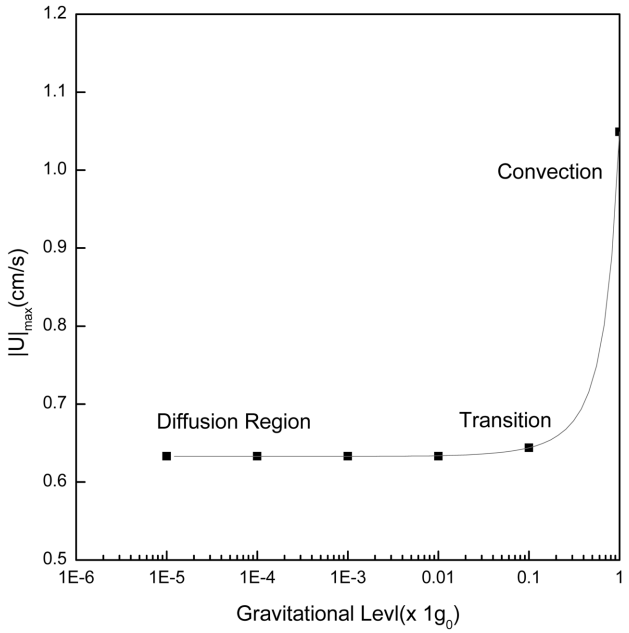

Fig. 11. Effects of gravitational level, g on the crystal growth rates of Hg_2Cl_2, for $1.0 \times 10^{-5}g_0 \le g \le 1g_0$. Based on $P_B = 300$ Torr, $\Delta T = 100$ K, Ar = 5, L = 10cm, and $T_s = 350^oC$, with linear temperature walls and thermo-solutal convection.

y = 0.5, and the maximum regions are slightly positioned into the left region from the centerline, which is likely to be due to the convection flow pattern. On the other hand, for $g = 0.1g_0$, the pattern is relatively well-balanced against y = 0.5, it indicates the diffusion would be predominant. Figs. 12 and 13 are based on the linear temperature profiles and thermo-solutal convection, P_B = 300 Torr, ΔT = 100 K, Ar = 5, L = 10 cm and $T_s = 350^oC$, P_T = 693 Torr, Pr = 0.99, Le = 0.86, Pe = 3.14, C_v = 1.04, Gr = 7.04×10^3. Fig. 13 shows the effects of binary diffusivity coefficient, D_{AB} on the dimensional maximum velocity magnitude $|U|_{max}$ for $0.1 \le D_{AB} \le 0.6$, with linear temperature profiles and thermo-solutal convection, P_B = 10 Torr, ΔT = 50 K, Ar = 5, L = 10 cm and $T_s = 350^oC$. The $|U|_{max}$s are linearly and directly proportional to the binary diffusivity coefficient, D_{AB} for both $1g_0$ and $0.1g_0$. The $|U|_{max}$s for $1g_0$ are greater that for $0.1g_0$ by a difference of 0.5 cm/s in $|U|_{max}$ between $0.1g_0$ and $1g_0$. It implies the greater is the diffusion coefficient, the more is the mass transport increased. From the points of view of crystal growers, decreasing the binary diffusivity coefficient from 0.6 to 0.4, i.e., by a factor of 0.67 is more efficient than changing the gravitational level from $1g_0$ to $0.1g_0$, i.e., by one order of magnitude. For D_{AB} = 0.1, the $|U|_{max}$ is reduced by a factor of 0.46 decreasing the gravity level from $1g_0$ to $0.1g_0$. With increasing the D_{AB} from 0.1 up to 0.6, the reducing factors changes from 0.46 to 0.8.

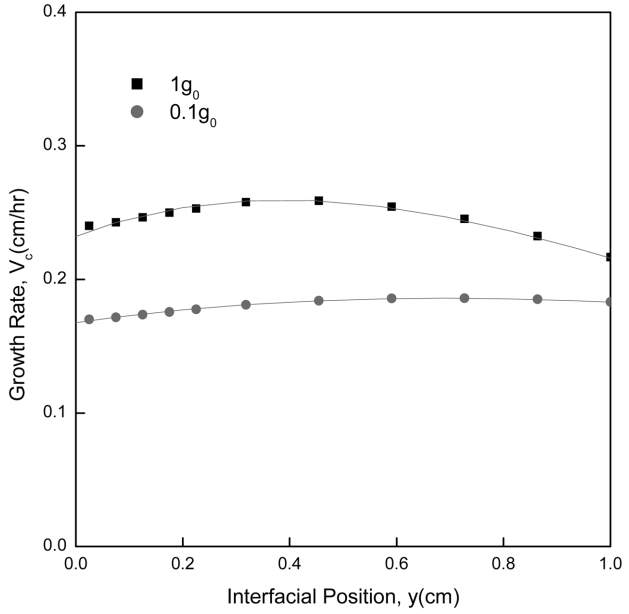

Fig. 12. Interfacial distribution of crystal growth rate of Hg_2Cl_2 for $0.1g_0$ and $1g_0$, corresponding to Fig. 11.

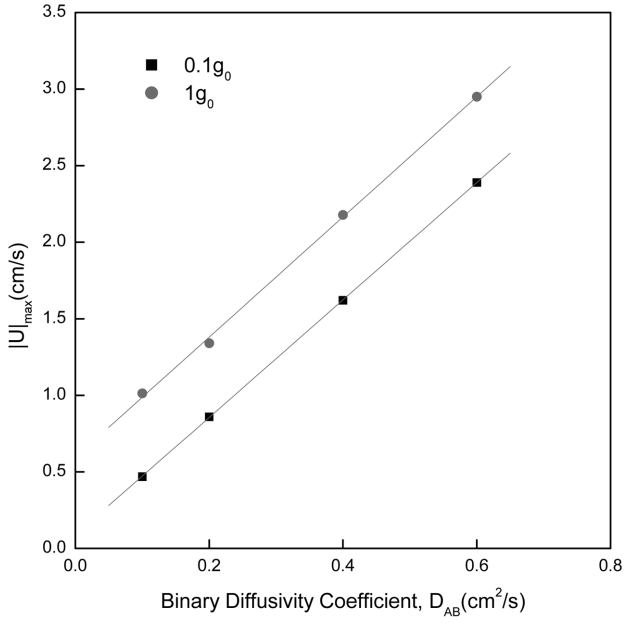

Fig. 13. Effects of binary diffusivity coefficient, D_{AB} (cm^2/s) on the crystal growth rates of Hg_2Cl_2 for $0.1g_0$ and $1g_0$. Based on P_B = 10 Torr, ΔT = 50 K, Ar = 5, L = 10 cm, and $T_s = 350^oC$, with linear temperature walls and thermo-solutal convection.

4. Conclusions

The parameters under consideration in this study are ΔT = 50 K, Ar = 5, P_B = 50 Torr, L = 5 cm, and $T_s = 350^oC$, the corresponding five dimensionless parameters of Pr = 1.12, Le = 0.2, Pe = 3.45, C_v = 1.03, Gr (Grashof number) = 2.42×10^3. It is concluded that for 10 K $\le \Delta T \le$ 50 K.

For 10 K $\le \Delta T \le$ 30 K, the growth rate slowly increases and, then is decreased gradually until ΔT = 50 K. The occurrence of this critical point near at ΔT = 30 K is likely to be due to the effects of thermo-physical properties stronger than the temperature gradient corresponding to driving force for thermal convection. Both the rates and the $|U|_{max}$s for the case of linear temperature profile are slightly greater than for the adiabatic walls for temperature ranges under consideration. For the range of 10 Torr $\le P_B \le$ 300 Torr, the rate is second order-exponentially decayed with partial pressures of component B, P_B. For 10 Torr $\le P_B \le$ 50 Torr, the rate is decreased significantly by the factor of 0.006, and for 50 Torr $\le P_B \le$ 300 Torr, reduced by a factor of 0.001. For the range of $5 \le M_B \le 200$, the rate is second order-exponentially decayed with a function of molecular weight of component B, M_B. The rate is decreased sharply for the range from M_B = 5 to 50 by a factor of 0.014, and then for $50 \le M_B \le 200$, is decreased by a factor of 0.0009. Like

the case of a partial pressure of component B, the effects of a molecular weight are reflected through the binary diffusivity coefficients, which are intimately related with suppressing the convection flow inside the growth enclosure, i.e., transition from convection to diffusion-dominant flow mode as the molecular weight of B increases. For the dimensional maximum velocity magnitude, $|U|_{max}$s, 1 g_0 g $10^{-5}g_0$, the convective mode is near at a ground level, i.e., on earth (1 g_0). The transition mode is switched from the convection to the diffusion mode for 0.1 g_0 g $10^{-2}g_0$, whereas the diffusion region ranges from $10^{-2}g_0$ up to $10^{-5}g_0$. The $|U|_{max}$s are linearly and directly proportional to the binary diffusivity coefficient, D_{AB} for both 1 g_0 and 0.1 g_0. The $|U|_{max}$s for 1 g_0 are greater that for 0.1 g_0 by a difference of 0.5 cm/s in $|U|_{max}$ between 0.1 g_0 and 1 g_0.

Acknowledgement

The authors wish to appreciate the financial support provided by the Hannam University through the Hannam University-Kyobi program of research project number of 2008A077 (April 1, 2008 through March 31, 2009).

References

[1] N.B. Singh, M. Gottlieb, G.B. Brandt, A.M. Stewart, R. Mazelsky and M.E. Glicksman, "Growth and characterization of mercurous halide crystals: mercurous bromide system", J. Crystal Growth 137 (1994) 155.
[2] N.B. Singh, R.H. Hopkins, R. Mazelsky and J.J. Conroy, "Purification and growth of mercurous chloride single crystals", J. Crystal Growth 75 (1970) 173.
[3] S.J. Yosim and S.W. Mayer, "The mercury-mercuric chloride system", J. Phys. Chem. 60 (1960) 909.
[4] F. Rosenberger, "Fluid dynamics in crystal growth from vapors", Physico-Chemical Hydro-dynamics 1 (1980).
[5] N.B. Singh, M. Gottlieb, A.P. Goutzoulis, R.H. Hopkins and R. Mazelsky, "Mercurous Bromide acousto-optic devices", J. Crystal Growth 89 (1988) 527.
[6] B.L. Markham, D.W. Greenwell and F. Rosenberger, "Numerical modeling of diffusive-convective physical vapor transport in cylindrical vertical ampoules", *J.* Crystal Growth 51 (1981) 426.
[7] W.M.B. Duval, "Convection in the physical vapor transport process-- I: Thermal", J. Chemical Vapor Deposition 2 (1994) 188.
[8] A. Nadarajah, F. Rosenberger and J. Alexander, "Effects of buoyancy-driven flow and thermal boundary conditions on physical vapor transport", J. Crystal Growth 118 (1992) 49.
[9] H. Zhou, A. Zebib, S. Trivedi and W.M.B. Duval, "Physical vapor transport of zinc-telluride by dissociative sublimation", J. Crystal Growth 167 (1996) 534.
[10] F. Rosenberger, J. Ouazzani, I. Viohl and N. Buchan, "Physical vapor transport revised", J. Crystal Growth 171 (1997) 270.
[11] N.B. Singh, R. Mazelsky and M.E. Glicksman, "Evaluation of transport conditions during PVT: mercurous chloride system", PhysicoChemical Hydrodynamics 11 (1989) 41.
[12] F. Rosenberger and G. Müller, "Interfacial transport in crystal growth, a parameter comparison of convective effects", J. Crystal Growth 65 (1983) 91.
[13] M. Kassemi and W.M.B. Duval, "Interaction of surface radiation with convection in crystal growth by physical vapor transport", J. Thermophys. Heat Transfer 4 (1989) 454.
[14] W.M.B. Duval, "Convection in the physical vapor transport process-- I: Thermal convection:, J. Chem. Vapor Deposition 2 (1994a), 188.
[15] W.M.B. Duval, "Convection in the physical vapor transport process-- II: Thermosolutal convection", J. Chem. Vapor Deposition 2 (1994b), 282.
[16] R.B. Bird, W.E. Stewart and E.N. Lightfoot, "Transport Phenomena" (John Wiley and Sons, New York, NY, 1960).
[17] C. Mennetrier and W.M.B. Duval, "Thermal-solutal convection with conduction effects inside a rectangular enclosure", NASA Technical Memorandum 105371 (1991).
[18] S.V. Patankar, "Numerical Heat Transfer and Fluid Flow" (Hemisphere Publishing Corp., Washington D. C., 1980).
[19] N.B. Singh and W.M.B. Duval, "Growth kinetics of physical vapor transport processes: crystal growth of the optoelectronic material mercurous chloride", NASA Technical Memorandum 103788 (1991).
[20] C. Mennetrier, W.M.B. Duval and N.B. Singh, "Physical vapor transport of mercurous chloride under a nonlinear thermal profile", NASA Technical Memorandum 105920 (1992).
[21] G.T. Kim, "Convective-diffusive transport in mercurous chloride (Hg_2Cl_2) crystal growth", J. Ceramic Processing Research 6(2005) 110.